Vortex Dynamics on a Pitching Delta Wing

S. P. LeMay*
Wright Research and Development Center, Wright-Patterson Air Force Base, Ohio
and
S. M. Batill† and R. C. Nelson‡
University of Notre Dame, Notre Dame, Indiana

A study of the dynamic behavior of the leading-edge vortices on a delta wing undergoing oscillatory pitching motions is presented. A sharp-edged, flat-plate, delta wing having a sweep angle of 70 deg was used in this investigation. The wing was sinusoidally pitched about its one-half chord position at reduced frequencies ranging from $k=2\pi fc/u=0.05$ to 0.30 at root chord Reynolds numbers between 9×10^4 and 3.5×10^5, for angle-of-attack ranges of $\alpha=29$ to 39 deg and $\alpha=0$ to 45 deg. During these dynamic motions, visualization of the leading-edge vortices was obtained by injecting $TiCl_4$ through ports located near the model apex. The location of vortex breakdown was recorded using high-speed motion-picture photography. The motion-picture records were analyzed to determine the vortex trajectory and breakdown position as a function of angle of attack. When the wing was sinusoidally pitched, hysteresis was observed in the location of the breakdown position. This hysteresis increased with reduced frequency. The velocity of breakdown propagation along the wing and the phase-lag between model motion and breakdown location were also determined. Detailed information was also obtained on the oscillation of breakdown position in both static and dynamic cases.

Nomenclature

c = root chord length
f = pitching frequency, Hz
k = reduced frequency, $2\pi fc/u$
Re = Reynolds number, uc/v
t = time, s
u = freestream velocity
u_x = velocity component parallel to wing chord
x = distance from apex parallel with wing chord
α = angle of attack, deg
$\dot{\alpha}$ = pitch rate, rad/s
μ = reduced velocity, $u_x/(cf)$
τ = convective time unit, c/u (s)
v = kinematic viscosity of air
ω = angular velocity or circular frequency

Introduction

WHEN a delta wing is pitched, plunged, or undergoes some other type of unsteady motion, there is a time lag in the response of the vortex flow which can result in temporarily delayed vortex formation at low angles of attack or temporarily delayed vortex breakdown at higher angles of attack. By taking advantage of these unsteady effects, a high-performance aircraft might be able to perform certain maneuvers more quickly and efficiently. For delta wings undergoing cyclic motions, a hysteresis develops in the vortex flow relative to the static case which increases with the frequency or rate of the motion. The hysteretic behavior of leading-edge vortices was observed in the experiments of Lowson[1] and Lambourne and Bryer.[2,3] Other changes also occur in the vortex flow, which are not readily apparent in the steady case. In the following, some specific findings are presented from research which has been previously performed on unsteady vortex dynamics. Most of the data were obtained from observations made through the use of flow visualization.

When investigating the response of the vortex flow on a delta wing due to periodic motion, a reduced frequency is typically defined as $k=\omega c/u$. However, alternate definitions are also used. To aid in comparison, all references to reduced frequency from other investigations have been converted to the definition used in this study.

Gad-el-Hak and Ho[4] sinusoidally pitched a 45-deg sweep delta wing, with a rounded leading edge, about the quarter-chord position from 0 to 30 deg at reduced frequencies ranging from 0.10 to 6.0. During the portion of the cycle in which the angle of attack was increasing, which is referred to as the upstroke, flow separation started at the trailing edge and propagated toward the apex. The propagation velocity of vortex-flow separation along the leading edge was approximately equal to that of the freestream velocity. During the decreasing angle of attack portion of the cycle or downstroke, they observed no distinct movement of the separation point along the leading edge; rather, the flow reattached along the entire leading edge at the same time.

Gad-el-Hak and Ho[4] also found the existence of a hysteresis in the vortex flow on a 45-deg sweep wing that was pitched between 10 and 20 deg in sinusoidal motion for chord Reynolds numbers of 2.5×10^4–3.5×10^5. The flow patterns at any particular angle of attack were very different on the upstroke and downstroke. The hysteresis was quantified from the growth and decay of the leading-edge vortex as the wing oscillated for reduced frequencies of $k=0.50$, 1.0, and 2.0. The size of the vortex, determined by the height of a dye marker above the wing at a specific x/c, was presented as a function of instantaneous angle of attack. At angles of attack of less than 15 deg, the hysteresis was not a function of reduced frequency. In this range of angle of attack, the hysteresis was the same for each reduced frequency. Also, the size of the vortex in the static case was approximately equal to the averaged values of vortex size on the upstroke and downstroke. At a reduced frequency of $k=0.50$, the average value (averaged between the upstroke and downstroke) of the vortex size followed the static case fairly well throughout the entire pitching cycle. A variation from this trend occurred as the reduced frequency was increased, and it was more evident at the higher angles of attack.

Received Nov. 3, 1988; revision received Aug. 22, 1989.

*First Lieutenant, U. S. Air Force, Flight Dynamics Laboratory. Member AIAA.
‡Associate Professor, Department of Aerospace and Mechanical Engineering. Associate Fellow AIAA.
‡Professor, Department of Aerospace and Mechanical Engineering. Associate Fellow AIAA.

This variation was because of the inability of the vortices to reach their fully developed size on the upstroke before the wing changed to downstroke.

Rockwell et al.[5] also reported the existence of a substantial hysteresis in the vortex flow relative to the static case. A 45-deg sweep delta wing, with a sharp leading edge, was pitched sinusoidally about its trailing edge from 5 to 20 deg at reduced frequencies of $k=0.16$ to 10.68. The chord Reynolds number was varied between 5.8×10^3 and 4.5×10^4. Hysteresis in the vortex flow became evident when the chordwise position of vortex breakdown was quantified as a function of instantaneous angle of attack. They found substantial hysteresis relative to the static case at a reduced frequency as low as $k=0.16$. The hysteretic behavior was generally the same for higher values of reduced frequency until a value of $k=1.75$ was attained. At $k=1.75$, the hysteresis effect started to reverse, and at reduced frequencies of $k=4.77$ and higher, the sense of the hysteresis was opposite to that of the $k<1.75$ cases.

Soltani et al.[6] obtained six-component balance data on a 70-deg delta wing sinusoidally oscillating between 0 and 55 deg at reduced frequencies of $k=0.015$ to 0.405. Dynamic forces and moments showed a significant overshoot at all reduced frequencies when compared to static data and were a strong function of pitch rate. Hysteresis loops were seen in all of the unsteady force balance results, and the amount of hysteresis increased with increasing reduced frequency.

Cunningham and den Boer[7] oscillated a straked delta wing in pitch throughout mean angles of attack -10 to 54 deg and amplitudes of 2 to 18 deg at frequencies from 0 to 16 Hz. The data that were analyzed included forces, pressures, and flow visualization results. They found an increasing lag tendency (compared to the steady case) in the normal force component at higher angles of attack and pitching frequencies, and the pitching moment data showed similar characteristics as well.

Gad-el-Hak and Ho[4] found that the effect of a Reynolds number on vortex flow was small. Two tests were conducted at Reynolds numbers of 2.5×10^4 and 3.4×10^5 and at a reduced frequency of $k=2.0$ for an angle of attack range of 0 to 30 deg. No measurable difference in the size of the vortices was observed between the two cases.

Gilliam et al.[8] pitched a delta wing at a constant pitch rate from 0 to 60 deg. For a 30-deg sweep, sharp leading-edge delta wing, the flowfield during pitching motion was characterized by a vortex structure, which was generated near the leading edge as the angle of attack increased and was then convected aft off the wing. The pitching rate primarily affected the length of time the vortex remained over the wing surface. The duration time decreased with increasing pitch rate; however, the vortex remained over the wing until higher angles of attack. Also, the vortex remained more coherent and its diameter increased with increasing pitch rate. No delay was detected in the response of the flow upon initiation of the pitching motion.

A similar experiment was performed by Reynolds and Abtahi[9] in which a delta wing of aspect ratio 1 was pitched at a constant rate, corresponding to a reduced frequency of 0.12. The wing was pitched about the one-half chord position from 30 to 51 deg and from 51 to 30 deg at four root-chord Reynolds numbers between 1.9×10^4 and 6.5×10^4. Large time lags associated with the location of vortex breakdown relative to the static case were observed, and a hysteresis was detected in the response of the vortex flow between the pitch-up and pitch-down cases. Another series of tests were conducted in which the wing was pitched down from an angle of attack of 51 to angles of attack varying from 45 to 20 deg. For these motions, the response times required for the breakdown location to reach a steady state, upon completion of the motion, were found to range from 1 to 30 convective time units. The convective time τ is the time required for the freestream flow to travel 1 chord length.

Gad-el-Hak et al.[10] observed that near the leading edge, there was a "roll up" of the shear layer, which formed discrete vortices along approximately straight lines originating from the apex for a static model. The discrete vortices were also observed in the unsteady case when the model was sinusoidally oscillated. However, in this case the discrete vortices were altered and modified by the unsteady motion, which had an order of magnitude lower frequency. Rockwell et al.[5] were able to attain active control of the leading-edge vortices for both large and small amplitude pitching motions by excitation of the shear layer, as observed by Gad-el-Hak and Blackwelder.[11]

This paper presents a study of the response of the vortex flow and breakdown location on a sinusoidally oscillating, 70-deg flat-plate delta wing with sharp leading edges, which was pitched about the one-half chord position. The effects of reduced frequency and Reynolds number were investigated. The reduced frequency was varied from $k=0.05$ to 0.30 for a root-chord Reynolds number of 2.6×10^5 and the Reynolds number was varied between 9×10^4 and 3.5×10^5 at a reduced frequency of $k=0.20$. The relatively low range of reduced frequency was selected because it is representative of the reduced frequencies experienced by the main wings on current high-performance aircraft.

Two angle-of-attack ranges of 29 to 39 deg and 0 to 45 deg were selected for testing. The smaller angle-of-attack range of 29 to 39 deg was chosen because throughout this range vortex breakdown occurs above the upper surface of the wing. Over this range of angle of attack, the breakdown location x/c varied from approximately 0.4 to 0.9. The larger amplitude motion of 0 to 45 deg provided information on the location of vortex breakdown at higher angles of attack. Statistical information on the oscillation of vortex breakdown position was also obtained.

Experimental Apparatus

Wind Tunnel

The wind tunnel used in this study was one of two identical low-turbulence, subsonic wind tunnels located in the University of Notre Dame Aerospace Laboratory. The tunnel is an in-draft, open-circuit design, which exhausts to the atmosphere. Additional information on the Notre Dame wind tunnel can be found in Ref. 12. The inlet of the tunnel consists of a 24:1 area contraction cone with 12 antiturbulence screens located just upstream of the inlet. The inlet configuration provides a near uniform freestream velocity profile in the test section with a turbulence intensity of less than 0.1%. The test section is 6 ft (183 cm) in length with a 2 ft $\times$ 2 ft (61 cm $\times$ 61 cm) cross section. The test section was constructed with large windows on the top and one side to provide a means of lighting and viewing the smoke tracer particles used in the flow visualization studies.

Model

A flat-plate delta wing model was used for all experiments in this study. The aluminum model was 1/2 in. (127 mm) thick with a leading-edge sweep of 70 deg and a trailing-edge span of 12 in. (305 mm). The root chord was 16.48 in. (419 mm). The leading edge was beveled symmetrically about the top and bottom surfaces of the wing at an inclination angle of 23 deg from the plane of the model. Smoke used for flow visualization was introduced into the flow through one of two ports located approximately 1 in. (25.4 mm) from the model apex and at the midline of the upper-surface bevel. The model was sting mounted and was free to pitch about a point located at the one-half root chord position 0.83 in. (21 mm) below the center of the model. The model was painted flat black to provide contrast for the white smoke used in flow visualization.

Unsteady Pitching Mechanism

A drive system was designed and fabricated to sinusoidally pitch the delta wing model with less than 2.5% harmonic distortion over the angle of attack range of 29 to 39 deg and less

than 5% harmonic distortion over the angle of attack range of 0 to 45 deg. The system was capable of oscillating the model throughout a wide range of reduced frequencies and amplitudes about a specified mean angle of attack. A schematic of the pitching mechanism is shown in Fig. 1, as it was mounted underneath the working section. Additional details on the pitching mechanism can be found in Ref. 12.

Flow Visualization

Titanium tetrachloride ($TiCl_4$) vapor was pumped from a specially designed thick-walled glass container using pressurized nitrogen gas. Nitrogen gas is an inert element with which $TiCl_4$ does not react. At standard room conditions, the liquid in the reservoir is easily vaporized because of the chemical's low vapor pressure. Therefore, as nitrogen is passed through the glass container, $TiCl_4$ vapor is taken with it. A piece of 3/16 in. (4.76 mm) i.d. tubing was used to deliver $TiCl_4$ vapor to the model with a 1/16 in. (1.59 mm) stainless steel probe attached to the end and mounted flush with the model surface. The flow of vapor was regulated using a needle valve located upstream of the $TiCl_4$ container.

Photographic Equipment

A Milliken DMB-5 16-mm motion-picture camera was used for the high-speed photography. A film frame rate of 64 frames/s (effective shutter speed 1/160 s) was used with Eastman 16-mm 4-X high-speed movie film. The model and smoke flow were illuminated using a 1000-W flood lamp placed above and upstream of the model. The camera was positioned to view along the pitching axis to provide a side view of the flowfield. By taking motion pictures from the side, the instantaneous angle of attack and chordwise vortex breakdown position were acquired.

Data Acquisition and Reduction

The photographic images were projected onto a digitizing table, and the resulting image was approximately 18×14 in. (46×36 cm). Five points (labeled A-E on the schematic in Fig. 2) were digitized to yield angle of attack and chordwise vortex breakdown location. Two points (A and B) were along the downstream side of the model sting in order to define a vertical reference vector, and two points (C and D) were at locations corresponding to the model apex and the center of the trailing edge respectively. Points C and D defined a vector lying along the root chord of the model. A fifth point, E, was then taken at the vortex breakdown location. This point was defined as the position at which the vortex core first appears to expand. This point was the most difficult of the five to locate accurately because of the nature of the breakdown phenomena. Breakdown does not occur at a single point but manifests itself as a rapid change in the diameter of the vortex core. The shape and form of the breakdown appeared to vary from frame to frame. In some frames a distinct expansion of the flow was clearly visible, whereas in others the expansion was more gradual. There was also a variability in quality of the smoke visualization which influenced the identification of the breakdown location. These factors contributed to the accuracy with which the breakdown location could be measured. Obviously, the measurement was somewhat subjective. However, after digitizing thousands of points, the experimenter becomes somewhat consistent in locating the breakdown location, and any bias that he may add is hopefully the same from frame to frame. An evaluation of the accuracy of the measurements was conducted, and it was estimated that measurements were repeatable within ± 0.3 deg for the angle of attack and within $x/c = \pm 0.01$ for the breakdown location.

A timing light was placed in the field of view of the motion-picture camera in order to indicate the start of each pitching cycle. The light was triggered by a microswitch on the gearbox that was engaged at a specific crank position and was used for ensemble averaging of the photographic data. A minimum of 8 complete pitching cycles were used for the ensemble average. The rms deviation in the breakdown location for the ensemble averaged data was typically 2% of the root chord.

Results

Vortex Breakdown over a Static Wing

To provide a reference for the unsteady cases, the vortex position was recorded using a pitch-pause technique for both increasing and decreasing angle of attack. The duration of the

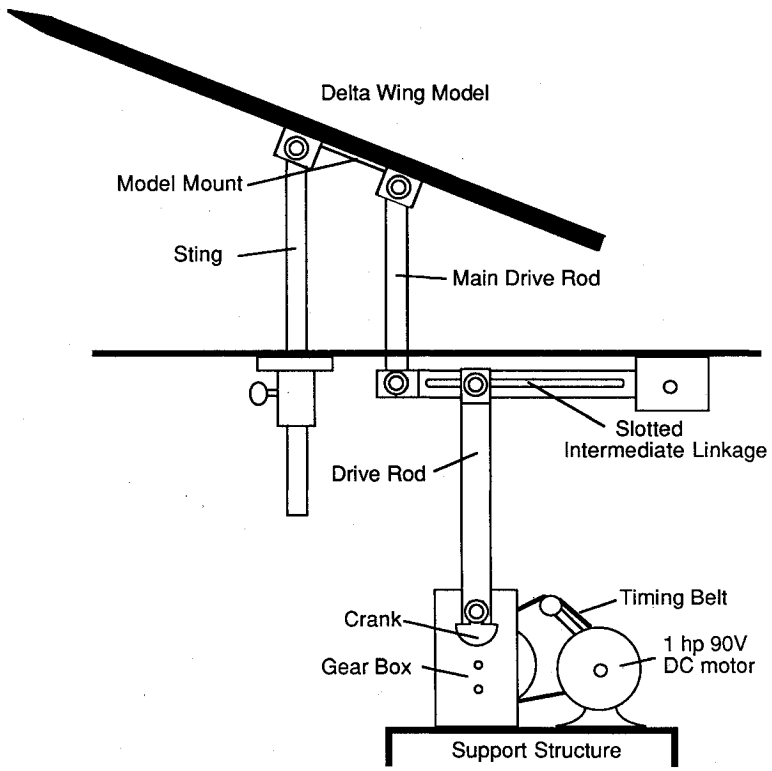

Fig. 1 Unsteady pitching mechanism.

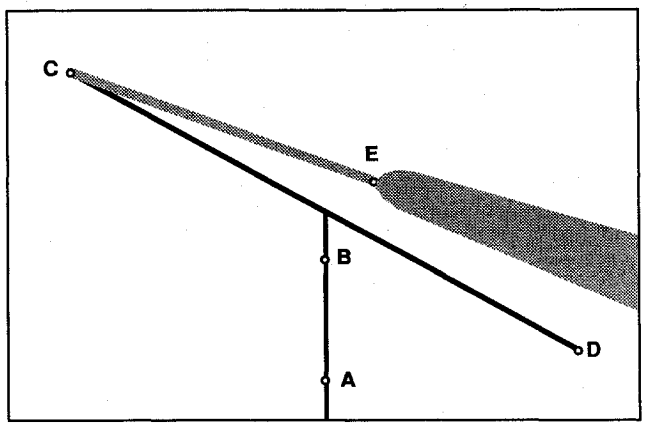

Fig. 2 Schematic of photographic data.

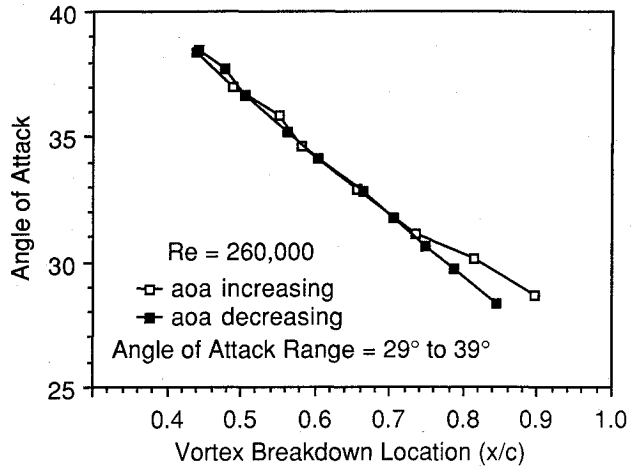

Fig. 3 Static chordwise location of vortex breakdown for increasing and decreasing angle of attack.

pause allowed the breakdown to achieve its nominal static position. The angle-of-attack range was 29 to 39 deg, the same as for the small amplitude dynamic cases. At each angle of attack recorded, an average breakdown location was computed using 10 photographic records, which spanned approximately 1.5 s of data. The static breakdown location was plotted as a function of angle of attack for both increasing and decreasing angle of attack, and the results are presented in Fig. 3. The curves are comparable at angles of attack above 31 deg, but below this value they deviate indicating a possible static hysteresis in this range of angle of attack. In this range, the breakdown location is farther downstream in the increasing α case than it is in the decreasing α case. Lowson[1] observed a similar phenomenon on an 80-deg sweep delta wing, for it took a lower static angle of attack to move the breakdown position into the wake of the model than it did to move it onto the trailing edge.

For the static model, there are fluctuations in the vortex breakdown location as identified using the visualization technique outlined above. Statistical information on the fluctuation of breakdown position for the static model was obtained. Breakdown point location was measured at a sampling rate of 64 Hz for 128 samples at both the minimum and maximum angles of attack. A discrete Fourier transform (DFT) was performed on the vortex breakdown position, and the rms variation in breakdown location was computed at each angle of attack. The average rms fluctuation about the mean was 1.3% of the root chord. Based on the number of samples and sampling rate, the DFT provided a frequency resolution of 0.5 Hz. There was no apparent dominant frequency in the breakdown point fluctuation in the range of 0 to 32 Hz for the static model.

Table 1

k	No. cycles averaged	Pitching frequency, Hz
0.05	8	0.174
0.10	8	0.347
0.20	20	0.694
0.30	9	1.042

$Re = 2.6 \times 10^5$, $\alpha = 29$ to 39 deg

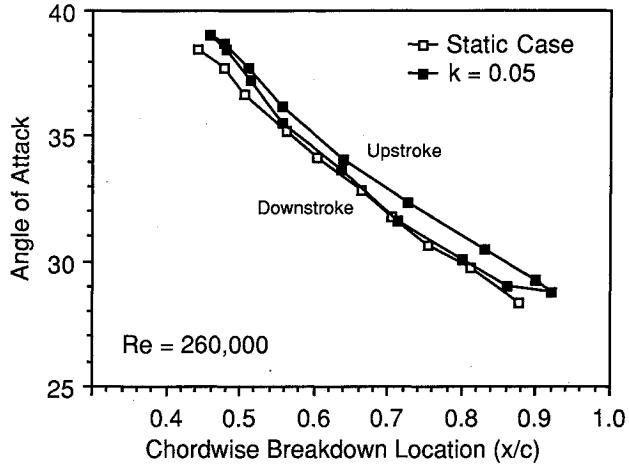

Fig. 4 Chordwise location of vortex breakdown, $k = 0.05$.

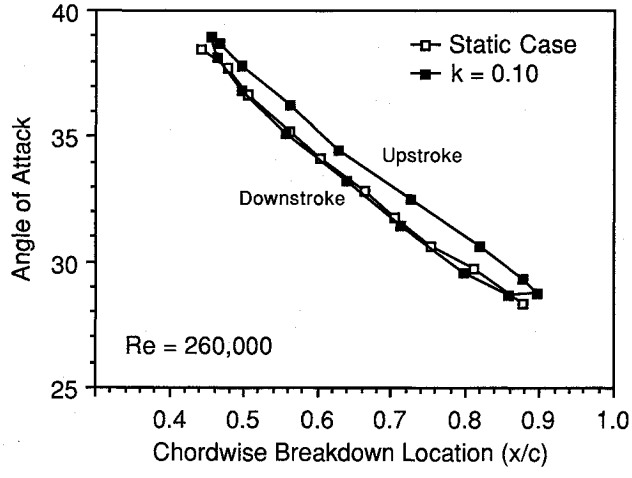

Fig. 5 Chordwise location of vortex breakdown, $k = 0.10$.

Vortex Breakdown Hysteresis

Four cases were investigated to determine the effect of reduced frequency on chordwise breakdown location over the angle of attack range of 29 to 39 deg at a constant freestream velocity of 30 ft/s corresponding to a root chord Reynolds number of 2.6×10^5. The four cases are summarized in Table 1.

Nondimensional chordwise breakdown location is plotted as a function of angle of attack in Figs. 4–7 for a pitching cycle along with static data obtained over the same angle-of-attack range and freestream velocity. The static data are averages of the increasing and decreasing static angle of attack cases shown in Fig. 4. Therefore the static hysteresis at the lower angles of attack is not shown.

At the lowest value of reduced frequency, $k = 0.05$, a hysteresis loop develops in the location of vortex breakdown. As the reduced frequency increases the hysteresis effect be-

comes greater at a given angle of attack. Also, the x/c range over which breakdown occurs decreases.

The decrease in the range of breakdown location is more apparent at the lower values of angle of attack where the breakdown position reaches its maximum x/c value. In this region, the maximum x/c value decreases from approximately 0.925 to 0.825 with increasing reduced frequency. At the higher reduced frequencies, the wing begins the pitch-up portion of the cycle before the breakdown position can reach its aftmost static location.

At the lowest frequency of $k=0.05$, an overshoot in the burst position past the static case is evident. This overshoot is slight and occurs at the minimum angle of attack. At the higher reduced frequencies, no overshoot occurs.

The resulting hysteresis loops become more symmetric about the static case as reduced frequency is increased. At reduced frequencies of $k=0.05$ and 0.10, the breakdown position lags the static case on the upstroke and is comparable to the static case on the downstroke. As reduced frequency is further increased to $k=0.20$, the amount by which the breakdown location lags the static case on the upstroke increases, and a similar lag begins to develop during the downstroke. At a reduced frequency of $k=0.30$, the hysteresis loop is nearly symmetric about the static data with the lag in breakdown position being approximately equal for both upstroke and downstroke phases of the pitching cycle.

Phase Difference Between Breakdown Location and Model Position

The phase-angle difference between chordwise breakdown location and model position was obtained for the dynamic cases presented in Figs. 4–7, in which the Reynolds number was constant at 2.6×10^5, and the reduced frequency varied between $k=0.05$ and 0.30 and for the cases where the reduced frequency was constant at $k=0.20$ and the Reynolds number varied between 9×10^4 and 3.5×10^5. A value for the phase lag was obtained by plotting both the breakdown location and model angular position against time for a cycle of motion. The phase angle was calculated graphically by determining the time difference between relative amplitude peaks.

In Fig. 8, the phase lag is plotted as a function of reduced frequency for a constant Reynolds number of 2.6×10^5. It is evident that a near-linear relationship exists between phase lag and reduced frequency. As the reduced frequency increases, so does the phase lag. The maximum phase lag is approximately 22 deg at the maximum reduced frequency of $k=0.30$. Maltby et al.[13] observed a phase lag in the vortex flow for a delta wing of aspect ratio 1 oscillating in heave at an incidence of 22 deg. They found a phase lag of 60 deg at a reduced frequency of 3.4, and 51 deg at a reduced frequency of 1.13.

Figure 9 illustrates the effect of Reynolds number on phase lag at a constant reduced frequency of $k=0.20$. The phase lag remains relatively constant for Reynolds numbers between 9×10^4 and 3.5×10^5. The maximum variation is approximately 2 deg, from a value of 15 deg at a Reynolds number of 9×10^4 to a value of 17 deg at a Reynolds number of 3.5×10^5. Therefore, a change in Reynolds number appears to have little effect on phase lag over the range investigated.

It is important to note that it is a change in the reduced frequency and not the pitching frequency that affects the phase lag. This point is illustrated in Fig. 10, where the phase lag is

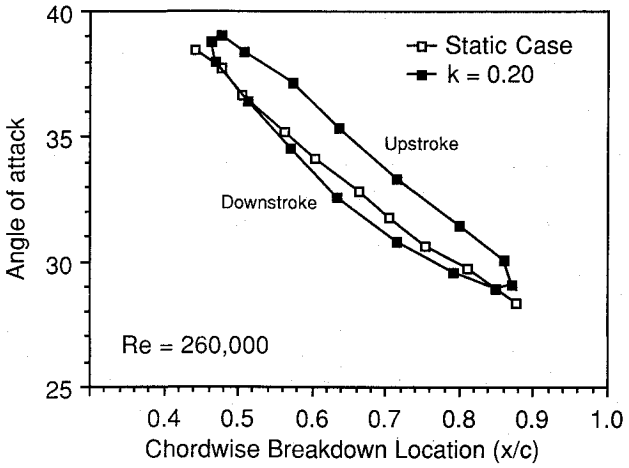

Fig. 6 Chordwise location of vortex breakdown, $k=0.20$.

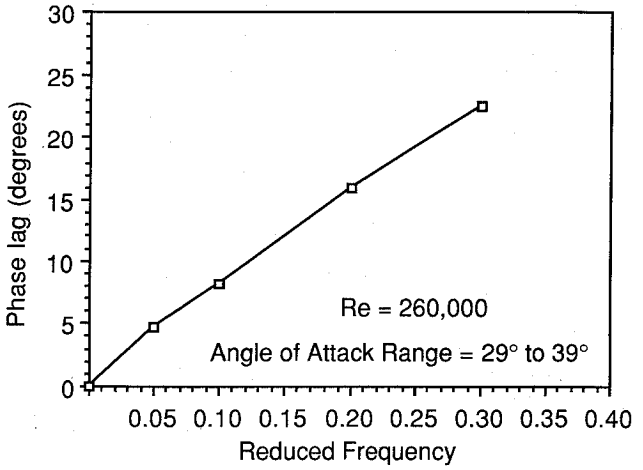

Fig. 8 Phase lag in the vortex flow as a function of reduced frequency.

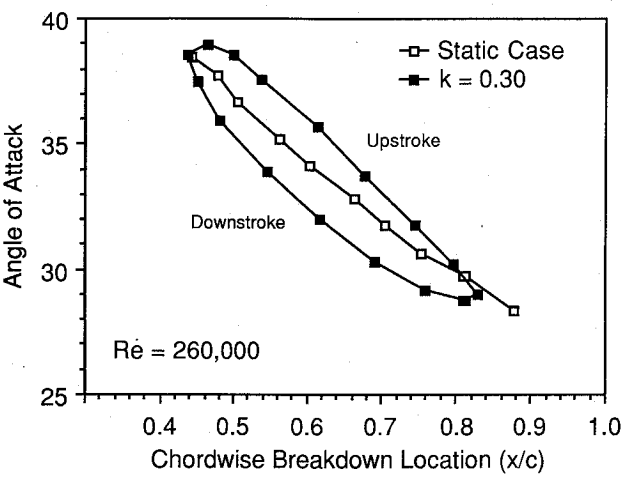

Fig. 7 Chordwise location of vortex breakdown, $k=0.30$.

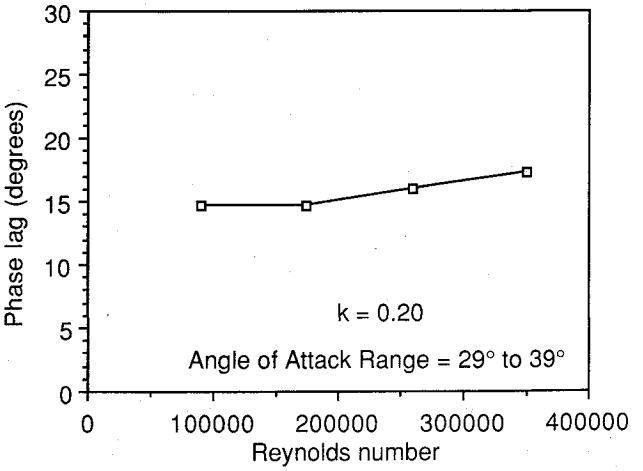

Fig. 9 Phase lag in the vortex flow as a function of Reynolds number.

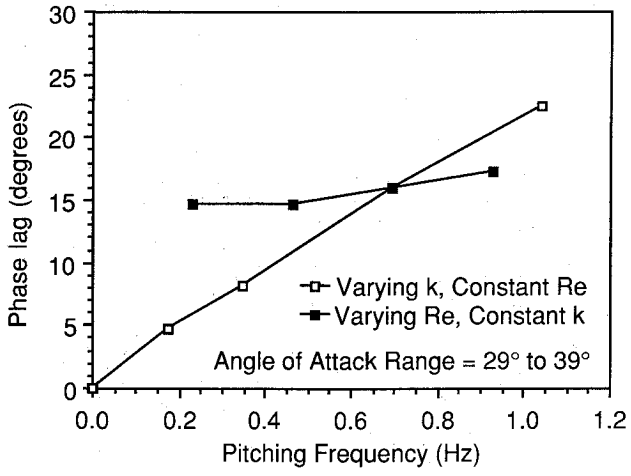

Fig. 10 Phase lag in the vortex flow as a function of pitching frequency.

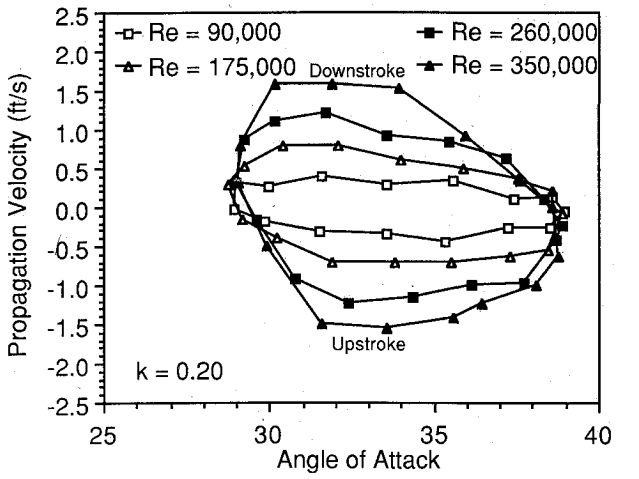

Fig. 12 Breakdown propagation velocity, $k=0.20$, $Re=9\times10^4$, 1.75×10^5, 2.6×10^5, and 3.5×10^5.

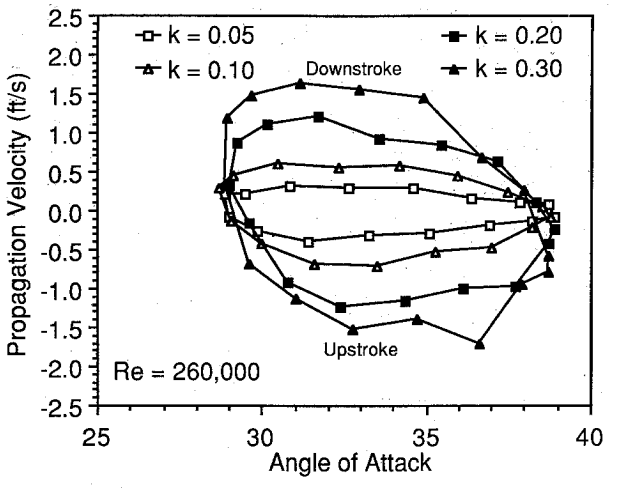

Fig. 11 Breakdown propagation velocity, $Re=2.6\times10^5$, $k=0.05$, 0.10, 0.20, and 0.30.

plotted against pitching frequency for both constant reduced frequency (varying Re) and constant Reynolds number (varying k). Both curves span approximately the same range of pitching frequencies yet are very different. The constant Reynolds number curve increases linearly with pitching frequency, whereas the constant reduced frequency curve increases only slightly.

Propagation Velocity of Breakdown Location

An approximation to the propagation velocity of vortex breakdown location relative to the delta wing was computed over a cycle of motion for each of the preceding small amplitude cases ($\alpha=29$ to 39 deg). The propagation velocity u_x was obtained by numerical differentiation of the chordwise breakdown location. The velocity was computed at the average x/c value of the data points used in the computation. A positive velocity corresponded to the breakdown location moving downstream, and a negative velocity corresponded to the breakdown position moving upstream. The process was repeated from data point to data point throughout the entire pitching cycle. The normal component of the propagation velocity was small in comparison to the axial component and was therefore neglected.

In Figs. 11 and 12, u_x was plotted against the angle of attack for varying reduced frequency and a constant Reynolds number of $Re=2.6\times10^5$ and for a varying Reynolds number and a constant reduced frequency of $k=0.20$, respectively. In Fig. 11, the magnitude of the velocity increases with reduced frequency with the maximum and minimum velocities being approximately equal for each case. The changes in velocity are more sudden at the lower angles of attack when the burst is closer to the trailing edge than at the higher angles of attack when the vortex breakdown is closer to the apex. The maximum velocity is attained in the angle of attack range of 30 to 32 deg on the downstroke, and the minimum velocity is attained in the angle of attack range of 31 to 33 deg on the upstroke. The maximum propagation velocity was 1.6 ft/s at a reduced frequency of $k=0.30$.

In Fig. 12, the Reynolds number is varied for a constant reduced frequency of $k=0.20$, and the magnitude of the velocity increases with the Reynolds number. Again, the maximum and minimum values of velocity are approximately equal for each of the cases, and the curves follow the same trends as the varying reduced frequency cases. A maximum velocity of 1.6 ft/s is attained at the highest Reynolds number of 3.5×10^5, which is approximately equal to 1/25 of the freestream velocity. The maximum velocities obtained in the other cases are also approximately equal to 1/25 of the corresponding freestream velocities.

The increase in breakdown point velocity observed in the two cases seems more dependent on pitching frequency than reduced frequency or Reynolds number. This is suggested by the fact that the range of pitching frequencies spanned is approximately equal in both cases, and the corresponding velocity plots are very similar. Thus, as the model is pitched with increasing angular velocity, the speed of breakdown propagation also increases. To eliminate this effect, a reduced propagation velocity (μ) is defined where $\mu=u_x/(cf)$. The data in Figs. 11 and 12 are replotted using reduced velocity and are shown in Figs. 13 and 14. From the plots, the influence of reduced frequency and Reynolds number can be seen.

The effect of reduced frequency is minimal throughout most of the pitching cycle as seen in Fig. 13, and the maximum reduced velocity in each case is approximately 1.2, which occurs in the angle-of-attack range of 30 to 33 deg. There appears to be little dependence upon reduced frequency except in the region at the beginning of the upstroke where the angle of attack starts increasing. More specifically, the change takes place between $\alpha=29$ and 35 deg. In this region the reduced velocity becomes more negative with decreasing reduced frequency. Therefore, the reduced velocity with which the burst moves up along the model increases. This increase is related to the shape of the hysteresis loops as illustrated in Figs. 3–7. Over the range of angle of attack in which this influence is observed, the location of vortex breakdown is further downstream in the lower reduced frequency cases, and the distance between data points is greater. This greater distance results in a higher value of reduced velocity.

The effect of Reynolds number on reduced velocity can be seen in Fig. 14. No distinct changes are apparent between the four cases. The maximum reduced velocity is approximately 1.2 in each case and occurs between 30 and 33 deg. Therefore, a change in Reynolds number has little influence on the reduced propagation velocity of breakdown location over the Reynolds number range of 9×10^4 to 3.5×10^5 at a reduced frequency of $k=0.20$. This is consistent with the insensitivity in breakdown position with Reynolds number observed by Lambourne and Bryer.[2,3]

Large Amplitude Oscillations

All of the previous results were for a relatively small range of angle of attack from 29 to 39 deg. Data for a larger amplitude motion, in which the wing was pitched from 0 to 45 deg, are presented in this section. Reduced frequencies of $k=0.05$ and 0.30 were investigated at a root chord Reynolds number of 2.6×10^5. The results are presented in terms of chordwise breakdown location and phase lag. However, the data included only that portion of the pitching cycle for which the breakdown was located above the wing. As the breakdown location moves into the wake, it leaves the camera's field of view and could not be measured. Because of this limitation, the velocity of breakdown propagation is not included.

The vortex breakdown location is plotted as a function of angle of attack in Fig. 15 for both reduced frequencies of $k=0.05$ and 0.30 at a Reynolds number of 2.6×10^5. A hysteresis is evident in both cases with the effect being much greater in the $k=0.30$ case. On the upstroke, the position of vortex breakdown is approximately the same for both cases at angles of attack greater than 32 deg. On the downstroke, however, a large variation occurs in the position of vortex breakdown. The breakdown location for the $k=0.30$ case lags the breakdown location of the $k=0.05$ case with the variation increasing with decreasing angle of attack. In the $k=0.05$ case, vortex breakdown moves into the wake at approximately 30 deg, and in the $k=0.30$ case, vortex breakdown moves into the wake at approximately 18 deg. Therefore, most of the hysteresis occurs during the downstroke phase over this range of angle of attack. The maximum hysteresis in breakdown location (while over the wing) occurs at approximately 30 deg for the $k=0.30$ case and at 31 deg for the $k=0.05$ case.

Soltani et al.[6] observed similar trends in force balance data acquired from a 70-deg delta wing, which was sinusoidally oscillated between 0 and 55 deg at reduced frequencies ranging from $k=0.015$ to 0.405. For each of the reduced frequencies considered, the normal force coefficients varied with reduced frequency. As the reduced frequency increased, the amount of hysteresis observed in the normal force increased. Therefore, most of the increase in the normal force hysteresis occurred during the downstroke phase of the cycle, as in the vortex breakdown location data presented in Fig. 15.

In Fig. 16, the breakdown location for the large amplitude case is compared to the breakdown location for the small amplitude case of 29 to 39 deg at the same reduced frequency of $k=0.30$ and Reynolds number of $Re=2.6\times10^5$. Also presented are the static data obtained for the small amplitude case. At any given angle of attack, the hysteresis effect is much

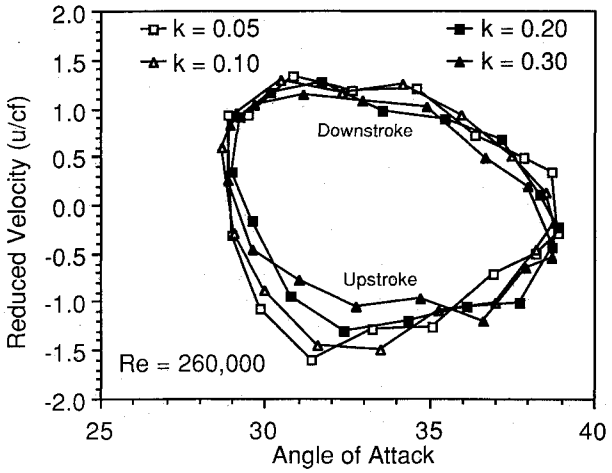

Fig. 13 Reduced breakdown propagation velocity, $Re=2.6\times10^5$, $k=0.05$, 0.10, 0.20,and 0.30.

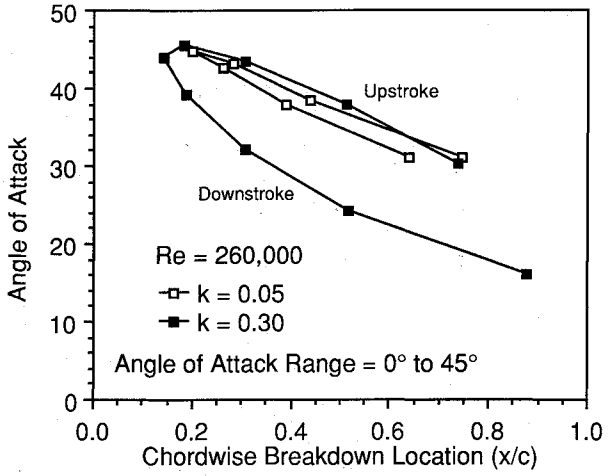

Fig. 15 Chordwise location of vortex breakdown, $k=0.05$ and 0.30, for $\alpha=0$ to 45 deg.

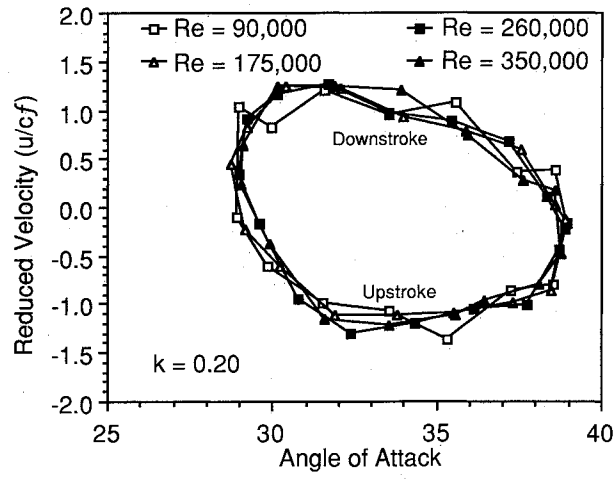

Fig. 14 Reduced breakdown propagation velocity, $k=0.20$, $Re=9\times10^4$, 1.75×10^5, 2.6×10^5, and 3.5×10^5.

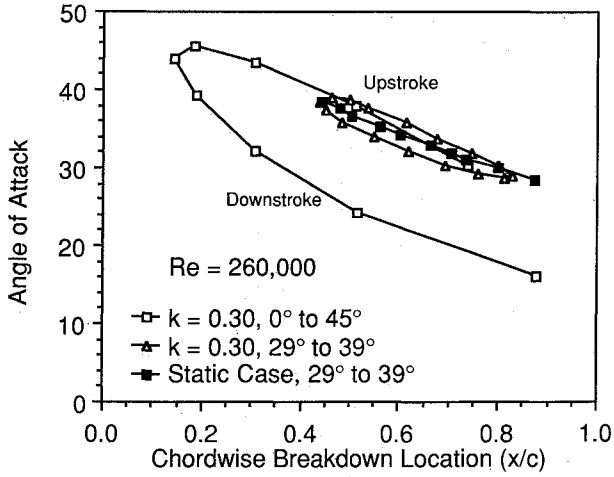

Fig. 16 Chordwise location of vortex breakdown, $k=0.0$ and 0.30 for $\alpha=0$ to 45 deg and 29 to 39 deg.

greater in the large amplitude case. Again, the large change occurs in the decreasing angle-of-attack portion of the cycle, and the static data lie much closer to the increasing angle-of-attack portion for the large amplitude case.

A phase lag for the vortex flow was computed through graphical means as for the small amplitude cases. Vortex breakdown location and model angular position were plotted as a function of time and the horizontal distance between the maximum angle of attack and minimum breakdown location was measured to provide the phase information. Minimum angle of attack could not be used as in the small amplitude case because at that position the flow was attached and vortex breakdown did not occur.

The phase lag in the $k=0.05$ case is 5 deg, and the phase lag in the $k=0.30$ case is 20 deg. These values are very similar to the phase lags obtained in the 29 to 39 deg cases for the same reduced frequencies and freestream Reynolds number. The values obtained in the small amplitude cases were 5 and 22 deg for reduced frequencies of $k=0.05$ and 0.30, respectively.

Finally, some preliminary tests were conducted to examine what influence, if any, a change in pitching axis had on the location of vortex breakdown. Three tests were performed with the pitching axis located at the one-quarter, one-half, and three-quarter chord locations for a reduced frequency of $k=0.30$ and a root chord Reynolds number of 2.6×10^5. As the pitching axis was moved toward the trailing edge, the average location of vortex breakdown also moved aft. This shift in breakdown location occurred throughout the entire pitching cycle. Moving the pitching axis from the one-quarter to one-half chord location resulted in moving the breakdown location x/c by approximately 0.04, and an equal amount of change was observed when the pitching axis was moved from the one-half to three-quarter chord position. Additional tests will be required to fully evaluate the influence of the pitch axis.

Conclusions

As the delta wing was oscillated in a sinusoidal fashion in the angle-of-attack range of 29 to 39 deg at reduced frequencies of $k=0.05$ to 0.30, a hysteresis developed in the chordwise position of vortex breakdown. A hysteresis is observed in the chordwise position of vortex breakdown at a reduced frequency as low as $k=0.05$. As the reduced frequency is further increased, the hysteresis effect becomes greater. At a given angle of attack, the distance between the position of vortex breakdown on the upstroke and the downstroke increases, and the maximum x/c position attained by vortex breakdown during the motion decreases. An overshoot in breakdown location past the static case was also observed in the $k=0.05$ case.

The phase lag in the position of vortex breakdown relative to the angular position of the wing was also calculated. The phase lag increases linearly with reduced frequency, and the maximum phase lag observed was approximately 22 deg at a reduced frequency of $k=0.30$ for a freestream Reynolds number of 2.6×10^5.

A reduced propagation velocity $\{u_x/(cf)\}$ of breakdown location was computed for varying reduced frequency and varying Reynolds number as well. In each case, the maximum reduced velocity obtained is approximately equal to ±1.2. This occurs over the angle-of-attack range of 30 to 33 deg. As with the phase angle, a change in Reynolds number was found to have little effect on the reduced velocity. A change in reduced frequency also had little effect except in the part of the pitching cycle where angle of attack started to increase after the model passed through minimum angle of attack. Here the magnitude of the reduced velocity increased with decreasing reduced frequency.

The average rms variation of the breakdown location x/c, obtained at discrete angles of attack throughout the pitching cycle for all cases investigated, was found to be 0.022. This is 70% greater than the average rms variation obtained for the static case over the same angle of attack range. In the static case, the frequency content of the breakdown point oscillation was determined at the maximum and minimum angles of attack of 29 and 39 deg. No dominant frequency or harmonics were apparent for either case.

When the wing was pitched through a large amplitude motion of 0 to 45 deg for reduced frequencies of $k=0.05$ and 0.30, a hysteresis develops in the location of vortex breakdown similar to that in the small amplitude cases. A hysteresis is evident at a reduced frequency as low as $k=0.05$, and at a reduced frequency of $k=0.30$, the effect is much greater. The most significant hysteresis occurs on the downstroke phase of the cycle.

A phase lag was also computed between the position of vortex breakdown and model angular position. The resulting phase lags are approximately equal to those obtained in the small amplitude case given the same reduced frequencies. Phase lags of 5 and 22 deg are obtained at reduced frequencies of $k=0.05$ and 0.30, respectively.

The complex behavior of the vortex breakdown during unsteady maneuvers will continue to be of concern, and both additional experiments and analytical model development will be necessary in order to improve our understanding of this phenomena.

Acknowledgments

This work was supported by the Department of Aerospace and Mechanical Engineering, University of Notre Dame and the NASA Langley Research Center, under Grant NAG 1-727, Jay Brandon, NASA Technical Officer. The authors gratefully acknowledge Roger Davis and Kenneth Visser for their contributions to the experimental facility development, and Scott Thompson for his help in reducing the photographic data.

References

[1]Lowson, M. V., "Some Experiments with Vortex Breakdown," *Journal of the Royal Aeronautical Society,* Vol. 68, 1964, pp. 343-346.

[2]Lambourne, N. C. and Bryer, D. W., "Some Measurements in the Vortex Flow Generated by Sharp Leading Edge Having 65 Degree Sweep," British Aeronautical Research Council, London, ARC CP 477, 1960.

[3]Lambourne, N. C. and Bryer, D. W., "The Bursting of Leading-Edge Vortices—Some Observations and Discussion of the Phenomenon," British Aeronautical Research Council, London, ARC R&M 3282, 1962.

[4]Gad-el-Hak, M. and Ho, C. M., "The Pitching Delta Wing," *AIAA Journal,* Vol. 23, No. 11, 1985, pp. 1660-1665.

[5]Rockwell, D., Atta, R., Kuo, C.-H., Hefele, C., Magness, C., and Utsch, T., "On Unsteady Flow Structure from Sweep Eddies Subjected to Controlled Motion," F. J. Seiler Research Lab., TR-88-0004, USAF Academy, CO, Sept. 1988, pp. 299-312.

[6]Soltani, M., Bragg, M., and Brandon, J. M., "Experimental Measurements on an Oscillating 70° Delta Wing in Subsonic Flow," AIAA Paper 88-2576, June 1988.

[7]Cunningham, A. M. and den Boer, R. G., "Harmonic Analysis of Force and Pressure Data Results for an Oscillating Straked Wing at High Angles," AIAA Paper 87-2494, Aug. 1987.

[8]Gilliam, F., Wissler, J., Robinson, M., and Walker, J., "Visualization of Unsteady Separated Flow About a Pitching Delta Wing," AIAA Paper 87-0240, Jan. 1987.

[9]Reynolds, G. A. and Abtahi, A. A., "Instabilities in Leading-Edge Vortex Development," AIAA Paper 87-2424, Aug. 1987.

[10]Gad-el-Hak, M., Ho, C. M., and Blackwelder, R. F., "A Visual Study of a Delta Wing in Steady and Unsteady Motion," *Proceedings of the Workshop on Unsteady Separated Flows,* edited by M. S. Francis and M. W. Luttges, Univ. of Colorado, Colorado Springs, CO, Aug. 1983, pp. 45-51.

[11]Gad-el-Hak, M. and Blackwelder, R. F., "The Discrete Vortices from a Delta Wing," *AIAA Journal,* Vol. 23, No. 6, June 1985, p. 961.

[12]LeMay, S. P., "Leading Edge Vortex Dynamics on a Pitching Delta Wing," M.S. Thesis, University of Notre Dame, Notre Dame, IN, April 1988.

[13]Maltby, R. L., Enger, P. B., and Keating, R. F. A., with Addendum by Moss, G. F., "Some Exploratory Measurements of Leading-Edge Vortex Positions on a Delta Wing Oscillating in Heave," British Aeronautical Research Council, London, R&M 3176, July 1963.